Fig. L.9.1 Relative change in HRS signals intensity of the AgNPs upon addition of the salts. (Incident laser power at 800nm: 50mW).

Fig. L.9. 2 HRS and continuum spectra of Ag NPs upon addition of 50mM NaCl. (Laser power at 800nm: 50mW). Also shown are spectra for bare and LiCl added AgNPs and the transmission curve of the bandpass filter used.

Contributed by:
K. Das; kaustuv@cat.ernet.in

L.10 Development of a handheld probe for real time imaging using optical coherence tomography

Optical coherence tomography (OCT) has emerged as an attractive technique for real time depth resolved cross-sectional imaging of biological tissues with micrometer-scale resolutions. OCT relies on the principle of low coherence interferometry, wherein light from a broadband source backscattered from a sample is mixed with the reference light using Michelson interferometer geometry. Interference takes place only when the sample arm path length matches exactly the reference arm path within the coherence length of the source. This allows probing different layers of the sample. Two-dimensional cross sectional imaging is achieved by performing successive axial measurements at different transverse positions. Previously a single mode fiber optic based optical coherence tomography system has been developed at Laser Biomedical Applications & Instrumentation Division, which is being used for in-vitro and in-vivo imaging of biological tissues. This setup can take axial scans at the rate of ~1Hz leading to typical image acquisition time of a minute or so. In order to acquire OCT images at video rate, a high speed OCT setup was developed with 1310nm broadband light source. The diode output was coupled into a fiber optic based Michelson interferometer by use of a 3-dB bi-directional fused fiber coupler designed for the wavelength used. The reference arm consists of a Fourier domain rapid scanning optical delay line using a resonant scanning mirror oscillating at 2KHz. Lateral scanning was done using a galvo scanner. The sample arm was designed to be in the form of a hand-held probe. The light incident on the galvo scanner was relayed with a pair of lenses and focused on to the sample using an objective lens. The light reflected from both the sample and reference arms was detected by a photodiode and the resulting interferogram was filtered and demodulated using a logarithmic amplifier and digitized using a frame grabber board. Two-dimensional OCT images were formed by lining up successive axial (depth) -scans and 2-D images were displayed on PC. Data was acquired from both the forward and reverse scans with an effective axial scan rate of 4KHz. The setup was designed to acquire images at the rate of 8 frames/sec. The axial and lateral resolutions of the setup in free space were ~18μm. The hand-held probe as shown in the picture is easily accessible for imaging skin of the human body. This setup is expected to have potential clinical applications in dermatology.

Fig. L.10.1 Photograph of the hand held OCT probe for dermal imaging.

Contributed by:
K.Divakar Rao; kdivakar@cat.ernet.in

L.11 Trapping of micron sized objects near a free liquid surface

It is difficult to manipulate objects near a free liquid surface with conventional optical tweezers because of the limited working distance available with the high numerical aperture objectives used in optical tweezers. We have shown that the thermocapillary effect, which arises due to the changes in surface tension of free liquid surface by laser induced heating, can be exploited for such applications.

The approach exploits the fact that the trap laser beam focused at a free liquid surface, results in an axi-symmetric temperature distribution at the surface having a

central hot point. This causes an axi-symmetric surface tension variation with a central minimum. Consequently, the surface profile gets deformed because of interplay of thermocapillary surface waves and internal gravity waves. The liquid is pulled out from the centre of the heated region and the depletion in the central region results in formation of a pit (fig. L.11.1). A careful analysis of the surface tension forces at the deformed liquid surface along with optical forces exerted by the incident laser beam, shows that these can lead to stable trapping of object in an annular region about the laser beam axis. It is pertinent to note here that the radiation pressure induced deformation of liquid surface is also present here and is expected to lead to a small bulging of the liquid surface along the beam axis. But such effect will be negligible compared to thermocapillary effect. Trapping of 2µm polystyrene microspheres with a 1064nm cw Nd:YAG laser beam (~ 40mW), focused with a low numerical aperture (0.5microscope) objective, is shown in fig. L.11.2. The trapped microspheres were imaged with a 40X objective lens and CCD camera. As can be seen in fig. L.11.2(a), initially the microspheres are trapped in an annular region about the laser beam axis. However, because of the convection flow, more microspheres are driven to the trap volume leading to a gradual build up of a cluster of the polystyrene microspheres. This approach could also be used for trapping of glass micro-rods and human red blood cells. The ability to manipulate microscopic objects near free liquid surface may prove valuable for several studies like for example, studies of colloidal dynamics at liquid-air interface, studies on crystalline thin-film structure of biomolecules like cholesterol at air/liquid interface etc.

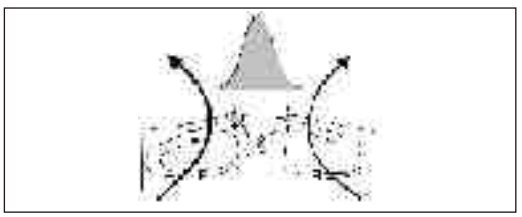

Fig. L.11. 1 *Trapping of microspheres at the free liquid surface, deformed by laser induced thermocappilarity. Dark arrows indicate optical forces and fade arrows indicate surface tension forces.*

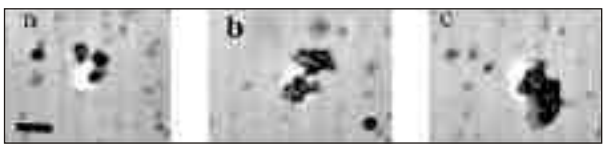

Fig. L.11.2 *Observation of trapping of 2µm polystyrene microspheres. (a) to (c) showing gradual accumulation of microsphers in the trap. Scale bar,10µm.*

Contributed by:
R. Dasgupta; raktim@cat.ernet.in, S. Ahlawat and P K Gupta

L.12 Active flux laser welding of austenitic stainless steel sheet

Active flux laser welding (ALW) process is being developed for austenitic stainless steel (SS) to produce narrower and deeper welds. The results of the laser welding (LW) study demonstrated that addition of flux (SiO_2) during LW caused significant reduction in the intensity and size of resultant plasma plume (fig. L.12.1). ALW was marked with large fluctuations in electron density of the plasma plume, which in turn, introduced fluctuations in the absorption of CO_2 laser radiation. ALW brought about significant modification in the shape of the fusion zones (FZ) to produce narrower and deeper welds than those made without flux. Flux-induced change in the shape of FZ was more marked in welds involving keyhole formation, although conduction-limited laser welds also carried signatures of flux-addition on its shape (fig. L.12.2). The most apparent difference in the case of deeper "ALW" welds was transformation of a typical "wine-glass" shaped fusion zones into a more uniformly tapered "V-shaped" fusion zones (fig. L.12.3). Active flux laser weldments exhibited lower ductility than those of bead-on-plate laser weldments.

Fig L.12.1 *Variation in plasma plume during laser welding of partly flux-coated SS sheet.*

Fig. L.12.2 *Comparison of conduction-limited welds produced by LW and ALW.*

Fig. L.12.3 *Comparison of key-hole welds produced by LW and ALW.*

Contributed by:
A. K. Nath; aknath@cat.ernet.in